On the corrections of ERA-40 surface flux products consistent with the Mediterranean heat and water budgets and the connection between basin surface total heat flux and NAO

D. Pettenuzzo (1) W .G. Large (2) N. Pinardi (3)

1. Istituto Nazionale di Geofisica e Vulcanologia, Bologna, Italy
2. National Center for Atmospheric Research, Boulder, Colorado
3. Bologna University, Corso di Scienze Ambientali, Ravenna, Italy

Abstract

This is a study of heat fluxes and heat budget of the Mediterranean Sea using the European Centre for Medium-Range Weather Forecasts (ECMWF) 45 year reanalysis data set ERA-40. The simple use of the ERA-40 surface flux components fails to close the budget and, in particular, the shortwave radiation flux is found to be underestimated with respect to observed data by about 10%. The heat flux terms are recomputed and corrected in order to close the heat and freshwater budgets of the Mediterranean basin over the period 1958 to 2001, thus producing a corrected ERA-40 surface flux data set. Various satellite and in situ observational data are used to construct spatially varying corrections to the ERA-40 products needed to compute the air-sea fluxes. The corrected interannual and climatological net surface heat and freshwater fluxes are $-7\ W/m^2$ and $-0.64\ \ m/yr$, respectively, which are regarded as satisfactorily closing the Mediterranean heat and water budgets. It is also argued that there is an important contribution from large heat losses associated with a few severe winters over the Mediterranean Sea. This is shown to be related to wind regime anomalies, which strongly affect the latent heat of evaporation that is the main responsible for the interannual modulation of the total heat flux. Furthermore, the surface total heat flux anomaly time series is compared with the North Atlantic Oscillation (NAO) index, and the result is a positive correlation with ocean warming for positive NAO index and cooling associated to negative index periods.

1 Introduction

The semi-enclosed nature of the Mediterranean basin plus ocean observations of the long term changes in Mediterranean heat storage and salt content offer the opportunity of calibrating and developing air-sea physics parametrizations so that an overall balance is attained between fluxes at the air-sea interface and lateral fluxes at Gibraltar. The so called "Mediterranean heat budget closure problem" [Castellari et al., 1998] states that the heat flux gained through the Gibraltar Strait by advection (considering the Black Sea contribution negligible [Tolmazin, 1985]) must be compensated, over a long enough period of time, by a net heat loss at the surface of the same amount while keeping the water budget of the basin reasonable. The heat inflow at Gibraltar has been estimated as $7 \pm 3\ W/m^2$ [Bethoux, 1979] and more recently as $5.2 \pm 1.3\ W/m^2$ [Macdonald et al., 1994]. The net surface water loss due to evaporation E and precipitation P over the basin has been estimated to be −1 m/yr [Bethoux and Gentili, 1994] while Gilman and Garrett [1994] indicate −0.71 ± 0.07 m/yr. Boukthir and Barnier [2000] determined a deficit of about 0.6 m/yr based on the ERA-15 reanalysis, and the range −0.5 to -0.7 m/yr is instead proposed by Mariotti and Struglia [2002]. Therefore, if the multiyear average surface heat and water fluxes from ERA-40 could be found to remain respectively within $-6 \pm 3\ W/m^2$ and between about −0.5 and −1.0 m/yr, we argue that they could be considered to satisfy the "Mediterranean heat budget closure problem". In order to evaluate the surface heat balance, oceanographers have used empirical bulk formulas together with atmospheric observations, sea surface temperatures and lately numerical weather prediction (NWP) surface fields. These attempts have failed to close the budget, giving positive values for the surface heat balance. Thus, rather ad hoc adjustments for biases have been applied. Garrett et al. [1992] estimated the surface heat balance using the COADS data set [Woodruff et al., 1987] from 1946 to 1988. To reduce the value obtained of $29\ W/m^2$ they suggested a possible reduction of the solar radiation

62 by a constant factor of 18%, or 33% more cooling by the latent and sensible heat fluxes. Later,
63 Gilman and Garrett [1994] proposed a modified set of formulae based on Garrett et al. [1992],
64 which reduced the solar radiation by approximately 9% by taking into account the attenuation of
65 incoming solar radiation due to atmospheric aerosol and increased the net cooling by long wave
66 radiation by about 15% based on preliminary measurements over the Tyrrhenian Sea. These
67 changes produced a surface heat balance of $0\ W/m^2$, and so still did not close the
68 Mediterranean heat budget. In another attempt, Castellari et al. [1998] intercompared different
69 air-sea flux formulae using the atmospheric NWP analyses and found the most appropriate ones
70 in order to obtain a negative surface heat balance for the Mediterranean Sea while maintaining
71 an acceptable water balance. They estimated a 1979-1988 mean value of $-11\ W/m^2$ for the
72 surface heat balance, and so again the Mediterranean heat budget was not closed. More recently
73 Tragou et al. [2003] demonstrated, using ground truth observations at several coastal
74 meteorological stations, that the incoming solar radiation is systematically overestimated by
75 $25\ W/m^2$ for the 30 years period which they considered (1964-1994), by the adopted empirical
76 formulation.
77 Many other techniques used to correct flux fields in different regions of the global ocean can be
78 found in literature, and a detailed review is included in the introduction of Large and Yeager
79 [2008]. They include assimilation of ocean observations [Stammer et al., 2004], inverse
80 procedures [Isemer et al. 1989], linear inverse analysis [Grist and Josey, 2003] and variational
81 objective analysis [Yu and Weller, 2007].
82 In this work we use an alternative approach based on the work of Large and Yeager [2008],
83 where spatially dependent correction factors are applied to the basic atmospheric fields required
84 as input to air-sea bulk formulae, including radiation. These correction factors are obtained by
85 comparison of the European Center for Medium Range Weather Forecast (ECMWF) Re-
86 Analysis fields (ERA-40, Uppala et al. [2005]) to satellite observations and in situ data sets
87 available for the period 1985-2001. The ERA-40 computed heat fluxes themselves do not solve

88 the “Mediterranean heat budget closure problem” in this period, but specific corrections to the
89 surface winds, sea surface temperature, radiative components and relative humidity values do
90 produce a satisfactory solution. The paper will then analyse the resulting time series in order to
91 explain how the surface heat balance is maintained and is correlated with the North Atlantic
92 Oscillation (NAO) index. We first introduce the air-sea physics notation and parametrizations
93 used in this study (section 2). In section 3 we will briefly describe the ECMWF ERA-40 fields
94 and discuss their implied surface heat and water balances. Section 4 describes the benchmark
95 data sets used for the bias reductions and the correction method. The resulting corrected fluxes
96 time series and climatology are presented in section 5, along with correlations with the NAO
97 index. A conclusion and discussion may be found in section 6.
98
99

2 Air-sea interaction physics

The surface heat balance gives the net heat flux at the air-sea interface Q_T as the sum of four dominant terms:

$$Q_T = Q_S + Q_L + Q_E + Q_H \qquad (1)$$

where Q_S is the net shortwave radiation flux, Q_L is the net longwave radiation flux, Q_E is the latent heat flux of evaporation and Q_H is the sensible heat flux. All fluxes have been taken positive for water or ocean energy gain. Both components of the radiative part of the heat balance are formed by the upward (negative) and downward (positive) fluxes, which are hereafter denoted by the subscripts U and D respectively:

$$Q_S = Q_{SD} + Q_{SU} = Q_{SD}(1-\alpha) \qquad (2)$$

$$Q_L = Q_{LU} + Q_{LD} = -\varepsilon\sigma T_S^{\,4} + Q_{LD} \qquad (3)$$

where T_S is the sea surface temperature, the ocean emissivity ε is taken to be 1 and σ is the Stefan-Boltzmann constant. When needed, a space-dependent albedo α following Payne [1972] is used.

The steady state Mediterranean water budget requires that the freshwater entering the basin through the Gibraltar Strait and from the Black Sea plus direct coastal runoff is lost through the surface.

The surface freshwater flux F_T is given by:

$$F_T = E + P \qquad (4)$$

where evaporation E is usually negative and precipitation P is positive definite.

The starting point of this work is the standard practice used by the Mediterranean Forecasting System (MFS) operational model (Pinardi et al. [2003], Tonani et al. [2008]).

The downward shortwave radiation is computed according to Reed [1977] and to Rosati and Miyakoda [1988].

125
$$\begin{aligned} Q_{SD}^{MFS} &= Q_{TOT}(1-0.62C+0.0019\beta) \qquad if \quad C \geq 0.3 \\ Q_{SD}^{MFS} &= Q_{TOT} \qquad if \quad C < 0.3 \end{aligned} \tag{5}$$

126 where Q_{TOT} is the total clear sky solar radiation reaching the ocean surface , C is fractional cloud
127 cover and β is the noon solar altitude in degrees.

128 For the longwave downward flux calculation, MFS uses the Bignami et al. [1995] formulation:

129
$$Q_{LD}^{MFS} = [\sigma T_A^4 (0.653 + 0.00535 e_A)](1 + 0.1762 C^2) \tag{6}$$

130 where T_A is the air temperature and e_A is the atmospheric vapor pressure [Lowe, 1977].

131 The turbulent fluxes (Q_H sensible and Q_E latent) are:

132
$$Q_H^{MFS} = -\rho_A C_P C_H \left|\vec{V}\right| (T_S - T_A) \tag{7}$$

133
$$Q_E^{MFS} = -\rho_A L_E C_E \left|\vec{V}\right| (q_S - q_A) = L_E C_E \tag{8}$$

134 where $\left|\vec{V}\right|$ is the wind speed, ρ_A is the density of the moist air, C_P is the specific heat capacity,
135 C_H and C_E are turbulent exchange coefficients for temperature and humidity, L_E is the latent
136 heat of vaporization, q_A is the specific humidity of air and q_S is the specific humidity saturated at
137 temperature T_S. In the MFS configuration, the exchange coefficients for a reference height of 10
138 m C_E and C_H are taken constant and equal to $1.5 \cdot 10^{-3}$ and $1.3 \cdot 10^{-3}$ respectively. These values
139 have been obtained from the wind speed dependent curves proposed by Kondo [1975]. In this
140 paper we use instead the approximated formula, suggested by the same author, which better
141 captures the wind speed dependent factors. The Kondo parametrization and its choice are
142 described and discussed in Appendix 1.
143
144

3 The ERA-40 surface heat budget

The ERA-40 data set covers the 45-year period from September 1957 to August 2002 with a time resolution of 6 hours. It is produced with a spectral atmospheric model based on a triangular truncation at wave number 156, which corresponds to a Gaussian grid of 1.125° (about 125 km). In the vertical, the ERA-40 atmospheric model has 60 hybrid levels with the highest at 0.1 hPa. The assimilation scheme used in ERA-40 is the three-dimensional variational (3D-Var) technique. It allows direct assimilation of raw radiances from TIROS Operational Vertical Sounder (TOVS) instruments. ERA-40 also uses SSM/I passive microwave data to analyze the total column water vapor and 10 m wind speed. Sea Surface Temperature (SST) and ice cover are taken from 2D-Var National Center for Environmental Predictions (NCEP) system and the Hadley Center respectively. Cloud motion winds are taken from geostationary satellites.
The parametrization of turbulent fluxes in the atmospheric model is based on the Monin-Obukhov similarity theory. The transfer coefficients depend on stability functions and differ from those used in the MFS system (Appendix 1). The roughness lengths for momentum, heat and moisture also include a free convection velocity scale, which represent the near surface wind induced by eddies in the free-convection regime. Further information can be found in Uppala et al. [2005].
For our purposes, all fields have been interpolated with a bi-linear algorithm to a regular 1/16 degree resolution grid. In such a process, the problem due to the influence of the land points on the ocean point values of the final grid has been taken into account. The original sea points have been extended over the land through a process called ”sea over land” which iteratively assigns to the first land value the average of the neighbouring sea points, before the interpolation is carried out. This methodology allows the production of a reference high-resolution corrected data set of surface fluxes in the Mediterranean basin assuming that seaward ERA-40 field values can be used to extrapolate in the near coastal areas. The interpolation does not add topographic effects

171 that are missing in the original ERA-40 data set but eliminates over-smoothing of the fields,
172 which will occur by simply interpolating across the coastal domain.
173 In this work we show that the simple usage of the surface flux components given directly by the
174 ERA-40 data set gives a lower than measured estimate of the net surface heat flux. The reason
175 for that is the underestimation of the shortwave radiation flux by about 12%, which is only
176 partially compensated by a less negative latent heat flux (see column 1; tab. 1). The ERA-40
177 solar radiation underestimation is evidenced by comparison with station surface radiation data
178 located in the Adriatic Sea (see figure 1) and the Sicily Strait. Figure 1 also compares the
179 downward shortwave flux from the International Satellite Cloud Climatology Project global
180 radiative flux data set (ISCCP-FD; Zhang et al. [2004]). The comparison supports the quality of
181 the surface radiation stations and the finding that ERA-40 is too low, by about $-20\ W/m^2$ in the
182 shortwave downward flux.
183 These results demonstrate that direct usage of ERA-40 fluxes to force an ocean general
184 circulation model for the Mediterranean Sea would be problematic [Griffies et al., 2008]. The
185 standard practice in ocean forecasting [Pinardi et al., 2003] is to calculate the surface fluxes with
186 the interactive bulk formulas (5), (6), (7) and (8) but this gives a very positive surface heat
187 balance ($24\ W/m^2$) (see column2; tab. 1). We need then to find a correction method to
188 recompute the heat fluxes from ERA-40 fields and close the Mediterranean heat budget.
189
190

4 Forcing fields bias reduction

In order to find a solution to the Mediterranean heat budget closure problem we use an approach based on the work of Large and Yeager [2008]: we correct the atmospheric fields and avoid using formulae for the computation of the radiative components of the surface flux. ERA-40 air temperature is not corrected because of the small impact that this correction would cause to the final heat budget value. The bias correction related to this field is estimated to be less than 1 °K and it would produce a total heat balance change smaller than 1 W/m^2.

The correction of the atmospheric fields is possible because of new observational data sets. However, some cover only a limited period of time with respect to ERA-40. For this reason we build up our correction methodology based on three steps:

- Step1: Observational data sets from various periods between 1985 and 2001 are used to determine objective corrections to ERA-40 products (see detailed descriptions on the following sections). These data sets are the QuickScat scatterometer (QSCAT) satellite wind fields [Chin et al., 1998], the satellite SST specifically analysed for the Mediterranean Sea [Marullo et al., 2007], the shortwave and longwave downward radiation (ISCCP-FD), the specific humidity from NOC climatology [Josey et al., 1998] and the CPC Merged Analysis of Precipitation (CMAP) [Xie and Arkin, 1996].
- Step2: We show that best estimates of the surface heat and freshwater fluxes do solve the Mediterranean heat budget closure problem, over the years 1985 through 2001. Since the QSCAT data are limited in time and NOC is a climatology, we only use them to correct ERA-40 winds and specific humidity, which with uncorrected ERA-40 air temperature, analysed SST, ISCCP-FD radiation and CMAP precipitation give the satisfying values of $-4\ W/m^2$ for the net surface total heat flux, and a deficit E+P of $-0.70\ m/yr$ (see column 7; tab.1). The adjustments computed in step 1 are then applied to the ECMWF reanalysis for the period 1985-2001, in order to verify that the resulting heat and

freshwater fluxes computed with what we will hereafter refer to as the "Corrected ERA-40 Data-set" still satisfy the "Mediterranean heat budget closure problem " constraint.

- Step3: Finally, we assume that the bias reduction corrections, obtained in the previous steps, are constant in time. Thus, they can be applied over the entire ERA-40 period (1958-2001) in order to produce a longer, consistent reference data set.

Some of the computed bias reduction terms are factors (denoted by the letter R: wind, shortwave radiation and precipitation), while others are differences (denote by the letter D: sea surface temperature and specific humidity). The corrections were computed using a linear regression between observed and ECMWF fields which evaluated slope (R) and offset (D) values. For the cases where the slopes were not significantly different from 1, only the additive parts were used, and conversely, only the ratios have been considered for the cases with a resulting offset value close to 0.

4.1 Wind speed correction

□□The advent of satellite wind products makes the ERA-40 wind speed validation possible. We utilize QSCAT (QuickScat Scatterometer) zonal U and meridional V wind components. These have been constructed 6-hourly on a half degree latitude-longitude grid, following Chin et al. [1998]. The ERA-40 wind speed is corrected by multiplying both its zonal U and meridional V components by a spatially-dependent factor. This correction factor is computed as:

$$R_W = \left\langle (U_Q^2 + V_Q^2)^{\frac{1}{2}} \right\rangle / \left\langle (U_{ERA}^2 + V_{ERA}^2)^{\frac{1}{2}} \right\rangle \qquad (9)$$

where $\langle\ \rangle$ denotes the average over the two years 2000 and 2001. In order to avoid problems with interpolations in coastal areas, the corrections have been applied only for values of R_W less than 1.3. There is no attempt to correct wind direction.□□Figure 2 shows the spatial distribution of the ratio R_W. A low bias is evident in the ERA-40 wind, with $R_W > 1$ everywhere, but smallest

242 in the south. The highest values are located in outflow regions of the major continental winds:
243 Mistral (Gulf of Lions), Bora (Adriatic Sea) and Ethesian (Aegean Sea). The overall effects of
244 the corrections are more cooling by the turbulent heat fluxes by about $22\ W/m^2$ and about
245 $0.25\ m/yr$ more evaporation. These are the largest single improvements made to the biases of
246 Table 1.
247

248 ## 4.2 SST correction

249

250 In order to reduce the SST bias, we use the OISST (Optimal Interpolated Sea Surface
251 Temperature) data set [Marullo et al., 2007]. Its resolution is daily on a 1/16 degree latitude-
252 longitude grid that matches the MFS OGCM grid for the Mediterranean basin. Unfortunately this
253 domain is smaller than the one of our basic forcing fields, so no SST corrections could be
254 computed for the Black Sea. The data set has been developed starting from satellite infrared
255 AVHRR images from 1985 to 2005, and has been validated with in situ measurements in order
256 to exclude any possibility of spurious trends due to instrumental calibration errors/shifts or
257 algorithms malfunctioning related to local geophysical factors. The validation showed that
258 satellite OISST is able to reproduce in situ measurements with a mean bias of less than 0.1 K and
259 RMS of about 0.5 K and that errors do not drift with time or with the percent interpolation
260 error. We compute the correction term for the period 1985-2001 as:

261 $$D_S = \langle OISST \rangle - \langle T_S^{ERA} \rangle \qquad (10)$$

262 where $\langle\ \rangle$ denotes the average over the 17 years, and the resulting space dependent correction
263 (figure 3) is added to the 6-hourly SST of ERA-40 T_S^{ERA}. The resulting time series is showed in
264 figure 7B. The sea surface temperature correction affects the longwave radiation Q_L, the latent
265 heat of evaporation Q_E and the sensible heat flux Q_H for a total contribution in the net surface
266 heat flux Q_T of $-4\ W/m^2$.
267

4.3 Radiation correction

Recent ISCCP (International Satellite Cloud Climatology Project) global radiative flux data products have been created by integrating the NASA Goddard Institute for Space Studies climate GCM radiative transfer model with a collection of global atmospheric data sets, including ISCCP clouds and surface properties [Zhang et al., 2004]. Most importantly, this ISCCP-FD data set provides fields of downwelling shortwave Q_{SD}^{ISCCP} and longwave Q_{LD}^{ISCCP} radiation as in equations 2 and 3. Moreover, since Q_{SD}^{ISCCP} and Q_{LD}^{ISCCP} have been derived in concert from the same input, they should derive full advantage of any cancellation of cloud errors. The data resolution is 3-hourly on a 2.5 degree longitude-latitude grid, but it is difficult to properly remap the diurnal cycle. Therefore, for our purposes, the data have been integrated to daily values and interpolated to the ERA-40 grid. Using these fields, we are now able to compute the ISCCP-FD net radiation from equations 2 and 3, which produces the values of columns 5, 6 and 7 in table 1. The solar heating is lowered by 19 W/m^2 compared to equation 5, but there is a partial compensation of about 8 W/m^2 from the longwave compared to equation 6. Note, the net short wave radiation flux of 183 W/m^2 from ISCCP-FD agrees with the proposal of Gilman and Garrett [1994], without making additional corrections for dust.

As described on step 2 of our correction methodology, in order to eliminate the bias that we could demonstrate exists on the ERA-40 radiation products, we have computed the ratio R_R as:

$$R_R = \left\langle Q_{SD}^{ISCCP} \right\rangle / \left\langle Q_{SD}^{ERA} \right\rangle \qquad (11)$$

where the two fields have been averaged for the period 1985-2001.

The resulting correction factor is shown in figure 4. The ISCCP-FD shortwave radiation is bigger than the ERA-40 one over the entire Mediterranean Basin with a strong North-West to South-East gradient and the largest errors occurring in the Levantine Sea. The corrected net shortwave radiation time series, obtained by monthly averaging the ECMWF radiation

multiplied to the factor R_R is represented in figure 8A.□□Regarding the long wave radiation component, the difference between Q_{LD}^{ISCCP} and Q_{LD}^{ERA} is less than 2% so an adjustment is not justified.

4.4 Specific humidity correction

The reference data set for this bias reduction is the NOC1.1 flux climatology, which is the renamed version of the Original SOC flux climatology [Josey et al., 1998]. The flux fields have been determined from in situ meteorological reports in the COADS 1a (Comprehensive Ocean Atmosphere Dataset 1a) covering the period 1980-93. A major innovation in the production of the climatology was the correction of the meteorological reports for various observational biases using additional measurement procedure information from the WMO47 list of ships.

In the MFS model implementation, the specific humidity is computed by the empirical formula:□□□□

$$q_A(T_D) = 0.98\rho^{-1}640.38e^{(-5107.4/T_d^{ERA})} \qquad (12)$$

where T_d^{ERA} is the ERA-40 dew point temperature given in °K and the 0.98 factor only applies over sea water. More accurate formulations are available, but not necessary, due to the uncertainty of the 0.98 factor and of the transfer coefficient C_E of equation (8), for instance.□□

However, the ERA-40 reanalysis atmosphere is drier than NOC, leading to the correction term shown in figure 5. It is the difference:□□□□

$$D_H = \left\langle q_A^{NOC} \right\rangle - \left\langle q_A^{ERA} \right\rangle \qquad (13)$$

where the two averages have been computed for the period 1980-1993.□□

After correction, ERA-40 reanalysis becomes wetter and the latent heat and evaporation are less negative by $9\ W/m^2$ and $0.11\ m/yr$, respectively. Again, in order to avoid errors as mentioned in section 4.1 we have limited the corrections to be no greater than $1.5\ g/m^3$. The monthly mean

surface averaged resulting specific humidity is shown in figure 7C.

4.5 Precipitation correction

With the above corrections and the uncorrected ERA-40 rainfall (given by the sum of large scale and convective precipitation) we obtain a deficit E+P of about -0.79 m/yr (see column 6; tab. 1). We decided to apply a further correction to the ECMWF reanalysis based on the CMAP data set [Xie and Arkin, 1996]. These are gridded fields of monthly precipitation obtained by merging estimates from five sources of information with different characteristics: gauge-based monthly analysis from the Global Precipitation Climatology Centre, three types of satellite estimates [the infrared-based GOES Precipitation Index, the microwave (MW) scattering-based Grody, and the MW emission-based Chang estimates], and predictions produced by the operational forecast model of the European Centre for Medium-Range Weather Forecasts (ECMWF). Figure 6 shows the ratio:

$$R_P = \langle P^{CMAP} \rangle / \langle P^{ERA} \rangle \qquad (14)$$

where the averages have been computed for the period 1979-2001. The ECMWF reanalysis precipitation is less over the northern Mediterranean basin, but more abundant over the southern. This last correction leads to a deficit E+P of -0.70 m/yr for the period 1985-2001, which is comparable to that obtained by Gilman and Garrett [1994] (even though their larger evaporation is compensated by more precipitation) and consistent with the results of Mariotti and Struglia [2002] who proposed -0.5 to -0.7 m/yr as the range for the excess of evaporation over precipitation.

5 Corrected heat and freshwater fluxes

In the previous section we have determined the field corrections, which produce the best estimates for heat and freshwater fluxes in the considered time window 1985-2001 (see column 7; tab. 1). At this point we assume that the space-dependent correction factors are constant in time and apply them over the entire ERA-40 reanalysis period (1958-2001).

The results are shown in table 2. In column 1, the flux components given directly in the original ERA-40 data set are presented. In column 2 we show those obtained with the "Corrected ERA-40 data set", calculated applying equations 2, 3, 7 and 8 using corrected ERA-40 shortwave radiation and uncorrected longwave radiation. Regarding the freshwater balance, both deficits E+P satisfy the values found in literature and cited in section 1, however the heat fluxes directly taken from ERA-40 fail to close the budget, according to the measurements of the heat gained through the Strait of Gibraltar ([Bethoux, 1979] and [Macdonald et al., 1994]). In the ECMWF reanalysis, the underestimation of the shortwave radiation flux is only partially compensated by less negative turbulent fluxes, such as the lower evaporation, which is redressed by a too low precipitation over the Mediterranean Basin. On the other hand, when we apply all the corrections and the new formulation for the radiative fluxes, the budget is recovered and the "Mediterranean heat budget closure problem" is solved. The budget has been evaluated also using the original resolution ERA-40 fields and the value of Q_T in Table 2 becomes $-5\ W/m^2$, a value still within the $6 \pm 3\ W/m^2$ uncertainty on the heat budget mean value.

An interesting effect of the corrections is the change in the balance of terms. The 17 W/m^2 increase in solar radiation is absorbed over a range of ocean depths, while the increased latent and sensible cooling is only from the surface. This shift in balance could have a profound effect on the seasonal cycle of SST, particularly during the spring heating and restratification season [Denman and Miyake, 1973].

5.1 Interannual variability

We now examine the interannual variability of the corrected heat balance components. Daily components have been calculated and then monthly averaged over the basin. The time series of monthly net shortwave radiation Q_S (figure 8A), obtained using equation (2) and the corrected Q_{SD} from ERA-40 data set, ranges from a winter minimum of 53 W/m^2 to a summer maximum of 302 W/m^2. It is dominated by a strong seasonal cycle with a small interannual signal, mostly due to the cloud coverage. In particular, the time series shows a summer cool anomaly during the years 1970-1973 which is due to an anomalous high cloud coverage during the same period (see figure 7D). The same effect is also evident in the net longwave radiation Q_L time series (figure 8B) where this term reaches its highest value of -60 W/m^2. In fact, since clouds have opposing effects on the two radiative components of the heat balance, there is a significant compensation between the two terms but again the effects on the SST will be different.

The sensible heat flux Q_H is the smallest of the four terms (figure 8D). It becomes positive during the months of April or May and remains negative for the remaining part of the year. It ranges from a maximum of 7 W/m^2 to a minimum value of -71 W/m^2 with strong interannual variability relative to its mean. There are five large minima during the years 1967, 1969, 1980, 1991 and 1999, which are related to strong wind regimes and air temperature anomalies during the same period (see figure 7).

The latent heat flux Q_E time series (figure 8C) is always negative, ranging from a summer maximum of -30 W/m^2 to a winter minimum of -130 W/m^2.

Finally, the surface total heat flux Q_T time series (figure 8E) shows a smooth signal dominated by the net short wave radiation flux and interannually modulated by Q_E and Q_H. It ranges from -275 W/m^2 to 181 W/m^2. However, it's important to notice that while the maxima of the time series, which occur during the months of May and June, show values which differ at most by about 30 W/m^2, the December minima can vary by more than 130 W/m^2. This peculiarity of

394 the Mediterranean basin plays a significant role in the climatological heat budget. Over the 44
395 years, replacing the 10 most negative values (the years 1962, 1967, 1968, 1969, 1980, 1986,
396 1990, 1991, 1995 and 1998) with the interannual average of the minima of the corrected Q_T
397 would change the overall mean from $-7\ W/m^2$ to about $-3.5\ W/m^2$. Since we pointed out that
398 the surface total heat flux is mainly interannually modulated by the latent heat of evaporation
399 and the sensible heat flux which are strongly affected by the wind regimes in the Mediterranean,
400 this means that the total heat budget is closed by approximately half of its long term value by
401 few strong cooling events due to cold and dry winds blowing over the basin during winter time.
402 This peculiarity proves the importance of choosing a long enough time window when one
403 attempts a budget study for this particular geographical area, since those extreme events have
404 necessarily to be included in the budget computation.
405

406 ## 5.2 Climatology

407

408 Figure 9 shows the pattern of climatological values of corrected Q_T for the months of July (A),
409 December (B), annual (C) and of annual F_T (D). These months also represent the maximum heat
410 loss and heat gain respectively. The heat flux annual mean shows minima in the north-western
411 Mediterranean (Gulf of Lion), in the Adriatic Sea and northern Ionian Sea, and in the Aegean
412 Sea, essentially reflecting the pattern of the principal continental winds (Mistral, Bora, Ethesian).
413 The maxima are instead located in the Alboran Sea, in the Channel of Sicily and in the Levantine
414 basin. Figure 9C shows a north-west to south-east pattern. Moreover, in areas of maxima the
415 summer heating (A) is much larger than winter cooling (B), while the opposite behaviour occurs
416 for the minima. The Southampton Ocean Centre (SOC) climatology [Josey et al., 1998] (not
417 shown) also provides a global estimate of surface heat and freshwater fluxes but over the
418 Mediterranean Sea its average heat flux of $42\ W/m^2$ is much larger than the measured heat
419 transport at Gibraltar. Nevertheless, the spatial pattern is similar to the corrected ERA-40

420 Q_T. The total freshwater flux (figure 9D) shows a strong north-south gradient, with small
421 areas where the precipitation exceeds the evaporation located on the northern coasts of the
422 Mediterranean basin.
423
424 ## 5.3 NAO changes and Mediterranean Sea net surface heat flux
425
426 The North Atlantic Oscillation (NAO) has been described as the indicator of the strength of the
427 zonal flow along the mid and high latitudes of the North Atlantic. The positive and negative
428 phases of the North Atlantic Oscillation are defined by the differences in pressure between the
429 persistent low over Greenland and Iceland and the persistent high off the coast of Portugal.
430 During a positive NAO phase both systems are stronger than usual, that is, the low has a lower
431 atmospheric pressure and the high has a higher atmospheric pressure. During the negative phase
432 of the NAO, both systems are weaker, lowering the difference in pressure between them. The
433 NAO is one of the major modes of monthly to interdecadal variability in the Northern
434 Hemisphere atmosphere, accounting for about one-third of the wintertime total variance. Interest
435 in the NAO has been recently renewed mainly because of a trend towards the positive phase of
436 the oscillation, particularly in the last two or three decades. In this section we explore the
437 Mediterranean-NAO teleconnection, which supposedly should be a dominant mode of variability
438 in the Mediterranean [Rixen et al., 2005]. After all, the ocean communicates with the overlying
439 atmosphere through changes in the heat fluxes. Moreover, heat flux is a more physically
440 meaningful parameter than the SST (see figure 10A for annual averages of Q_T).
441 For this reason, we compared the Winter (December through March) NAO index based on the
442 difference of normalized sea level pressure between Lisbon, Portugal and
443 Stykkisholmur/Reykjavik, Iceland, with the annual mean Q_T anomaly time series, computed as
444 the differences of the yearly mean total heat fluxes from the overall mean of -7 W/m^2 given in
445 Table 2. The sea level pressure anomalies at each station were normalized by division of each

446 seasonal mean pressure by the long-term mean (1864-1983) standard deviation. Normalization is
447 used to avoid the series being dominated by the greater variability of the northern station. The
448 station data were originally obtained from the World Monthly Surface Station Climatology.
449 Further details can be found in Hurrell et al. [2001]. The correlation coefficient that we
450 obtained between the two yearly time series is 0.37 with a 95% confidence interval of
451 $0.08<C<0.60$, which is very small, however, a similar oscillation at longer time-scales was
452 noticeable in the two curves (not shown). In order to quantify this information, we computed for
453 both Q_T anomaly and NAO index a five-year running mean, and we compared the two resulting
454 time series (figure 10B). The resulting correlation coefficient has the much more significant
455 value of 0.68 and a 95% confidence interval of $0.48<C<0.81$, meaning that the two fields have a
456 high positive correlation. We can argue that this relationship is at least partially due to the wind
457 regimes induced by the NAO itself: a positive index implies lower winds over the Mediterranean
458 Basin, which determines lower evaporation and consequentially a lower latent heat flux which is,
459 as we pointed out, the largest modulation factor of the net total surface heat flux. Conversely, a
460 negative NAO index is accompanied by a stronger wind regime over the basin, that implies
461 greater evaporation and as a direct consequence a low Q_T anomaly. Moreover, the climatological
462 nature of this correlation once again confirms the importance of the choice of a long period for
463 budget studies in the Mediterranean Sea, since the long time scale effects of the NAO must be
464 definitely taken into account because of their direct implication on the air-sea interaction heat
465 exchange processes.
466

6 Conclusions

In this paper we show that the Mediterranean Sea places a valuable constraint on the long-term mean basin averaged Q_T, which should compensate for the measured net heat inflow at Gibraltar. Furthermore, freshwater budget considerations constrain the evaporation and consequently the latent heat flux. These are aspects of so called "Mediterranean heat budget closure problem", which have been addressed by the data sets of this study.

We demonstrate that ECMWF ERA-40 reanalysis without any corrections to its surface fields does not close the budget. In addition, the individual components of the surface heat balance are incompatible with some in situ local observations (figure 1). For this reason, we adapted a correction method, developed by Large and Yeager [2008] for the global ocean, to the Mediterranean Sea. This method is based on the determination of the best estimate of the heat and freshwater budgets for a reference period chosen to match the availability of important reference data sets. For this period (1985-2001) we have computed different space dependent bias reduction terms which, when applied to the ERA-40 reanalysis forcing fields along with the use of a new formulation for radiative fluxes, allow the satisfaction of the Mediterranean closure problem. Averaged over the basin, they increase the shortwave radiation by $21\ W/m^2$, increase the wind speed by 25%, increase the specific humidity by about $1\ g/m^3$ and increase the sea surface temperature (SST) by less than 1°C. Locally the SST correction ranges from more than 2°C to about -1°C. The precipitation is increased by about a factor of 2 off some northern coasts and reduced along the southern and eastern margins where there is little rainfall. The correction terms have been then extended to the entire ERA-40 period (1958-2001). In this way, we have constructed what we called the "Corrected ERA-40 data set" that is an high frequency (6-hourly) data set suitable for forcing ocean models in the Mediterranean area. Recently the MFS model has been used as a test-bed to check the correction method for the atmospheric fields and air-sea physical parametrizations described in this paper. Preliminary results obtained during a one-year

493 integration experiment show an improvement in the estimation of the SST and a positive impact
494 on the model temperature and salinity profiles if compared with in situ data. The impact of air-
495 sea physical parametrizations on the model simulation quality will be an area of active research
496 in the near future.
497 Among all the corrections, that on wind speed has the largest effect ($-22\ W/m^2$) on the final
498 surface heat balance. Furthermore, the interannual modulation of Q_T is imposed by the latent
499 heat flux Q_E and the sensible heat flux Q_H (see figure 8) which are strongly dependent on the
500 wind speed and wind speed events during wintertime.
501 Shortwave radiation correction is also large for the ERA-40, probably due to the compensating
502 effects in the atmospheric model, which has produced it. Moreover, in situ and satellite data sets
503 confirm that the annual mean value should be about 180 W/m^2 as previously found by Gilman
504 and Garrett (1994).
505 Finally, the net surface heat flux Q_T is related to the winter NAO index. A correlation coefficient
506 of 0.68 has been found after a 5-year running mean filter has been applied to the two time series.
507 This aspect underlines the fact that the correlation is to be considered in a climatological sense.
508 In other words, NAO yearly variations are not directly correlated to annual mean heat flux
509 anomalies over the Mediterranean Sea but only the long time scale modulation can be associated
510 to teleconnections.
511 Wind anomalies during winter are responsible for half the negative heat budget of the basin. Our
512 study points out the need for longer time series of fluxes to really understand their low frequency
513 variability and to solve the heat budget closure problem.

Appendix 1: Bulk transfer coefficients

The bulk transfer coefficients used in this work for the computation of latent heat of evaporation and sensible heat fluxes (eq. 7 and 8) are taken according to Kondo [1975], who suggested the following approximate formulas for neutral stability, when the wind speed in expressed in m/s:

$$10^3 C_H(10m) = a_h + b_h\left|\vec{V}\right|^{p_h} + c_h(\left|\vec{V}\right| - 8)^2 \qquad (15)$$

$$10^3 C_E(10m) = a_e + b_e\left|\vec{V}\right|^{p_e} + c_e(\left|\vec{V}\right| - 8)^2 \qquad (16)$$

where the numerical constant $a_{h,e}$, $b_{h,e}$, $c_{h,e}$ and $p_{h,e}$ vary with a range of wind speed speeds as shown in Table 3. The coefficients for non-neutral cases are expressed in terms of a practical index of atmospheric stability, which are obtainable from wind speed and the difference of temperatures at the sea surface. Figure 11a shows C_E computed according to equation 16 for neutral condition (T_A-T_S=0) and for other 6 non-neutral cases (T_A-T_S=3.0, 2.0, 1.0, -1.0, -2.0, -3.0).

The formulation is obtained under the condition that no ocean spray exists. In strong wind regimes, it is almost certain that the effect of the ocean spray on the temperature and humidity profiles would be important thus leading to unrealistic coefficient values. This approximation is reasonable in the Mediterranean Basin where the average wind speed is about 6 m/s, however the previous equations are not used for wind speed greater than 50 m/s. This parametrization is used for consistency with the Mediterranean Forecasting System (MFS) standard air-sea physics which was calibrated in a comparison study between different bulk formulas (Castellari et al., 1998).

In order to provide an estimate of the sensitivity of our results on different exchange coefficients, we recomputed the total heat and freshwater budgets using an alternative parametrization. Figure 11b shows the coefficient obtained from the Coupled Ocean-Atmosphere Response Experiment (COARE) bulk algorithm (version 3.0) as described in Fairall et al. [2003] and then

539 expressed as polynomial functions by Kara et al. [2005]. These so-called NRL Air-Sea Exchange
540 Coefficients (NASEC) include stability dependence through air-sea temperature difference, wind
541 speed at 10 m above the sea surface and relative humidity.
542 Table 4 presents the total fluxes and their components computed at the original ERA-40
543 resolution using Kondo and NASEC parametrizations. The coefficients are about 10% different
544 at low wind speed and this produces a difference of 8 W/m^2 in the latent heat of evaporation and
545 1 W/m^2 in the sensible heat flux. This result confirms the choice of Kondo (1975) for the
546 Mediterranean Sea, which gives the value of 94 W/m^2 as suggested by Gilman and Garrett
547 (1994) with corrected atmospheric fields from ERA-40.

Acknowledgments

The OI-SST products used in this paper were jointly produced by ENEA Department of Environment, Global Change and Sustanable Development and Gruppo Oceanografia da Satellite (GOS) of the CNR - ISAC (Istituto di Scienze dell'Atmosfera e del Clima) as part of the EU project MFSTEP (EVK3-CT-2002-00075).

The National Center for Atmospheric Research is sponsored by the National Science Foundation.

The in situ AGIP data were kindly supplied by ENI-AGIP division, Milan.

References

Bethoux, J. P. (1979), Budgets of the Mediterranean sea; their dependence on the local climate and on the characteristics of the Atlantic waters, *Oceanologica Acta, 2*, 157–163.

Bethoux, J. P., and B. Gentili (1994), The Mediterranean Sea, a test area for marine and climatic interaction, *Ocean processes in climate dynamics, 46*, 239–254.

Bignami, F., S. Marullo, R. Santoleri, and M. E. Schiano (1995), Long wave radiation budget on the Mediterranean Sea, *Journal of Geophysical Research, 100*, 2501–2514.

Boukthir, M., and B. Barnier (2000), Seasonal and inter-annual variations in the surface freshwater flux in the Mediterranean Sea from the ecmwf re-analysis project, *Journal of Marine Systems, 24,* 343–354, doi: 10.1016/S0924-7963(99)00094-9.

Castellari, S., N. Pinardi, and K. Leaman (1998), A model study of air-sea interactions in the Mediterranean Sea, *Journal of Marine Systems, 14*, 89–114.

Chin, T. M., R. F. Milliff, and W. G. Large (1998), Basin-scale, high-wave number sea surface wind fields from a multiresolution analysis of scatterometer data, *Journal of Atmospheric and Oceanic Technology, 15*, 741–763.

Denman, K. L., and M. Miyake (1973), Upper layer modification at ocean station papa: Observations and simulation, *Journal of Physical Oceanography, 3*, 185–196.

Fairall, C. W., E. F. Bradley, J. E. Hare, A. A. Grachev, and J. B. Edson (2003), Bulk

parameterization of air-sea fluxes: Updates and verification for the COARE algorithm, *Journal of Climate*, 16, 571-591.

Garrett, C., R. Outerbridge, and K. Thompson (1992), Interannual variability in Mediterranean heat and buoyancy fluxes, *Journal of Climate, 6*, 900–910.

Gilman, C., and C. Garrett (1994), Heat flux parameterizations for the Mediterranean Sea: The role of atmospheric aerosol and constraints from the water budget, *Journal of Geophysical Research, 99*, 5119–5134.

Griffies, S., A. Biastoch, C. Boning, F. Bryan, G. Danabasoglu, E. Chassignet, M. England, R. Gerdes, H. Haak, R. Hallberg, W. Hezeleger, J. Jungclaus, W. Large, G. Madex, B. Samuels, M. Sheinert, C. Severijns, H. Simmons, A. Treguier, M. Winton, S. Yeager, and J. Yin (2008), Coordinated ocean-ice reference experiments (cores), *Ocean Modell, 11*, 59–74.

Grist, J. and S. Josey (2003), Inverse analysis adjustments of the SOC air–sea flux climatology using ocean heat transport constraints, *Journal of Climate*, 16, 3274–3295.

Hurrell, J. W., Y. Kushnir, and M. Visbeck (2001), The north Atlantic oscillation, *Science, 291*, 603-605.

Isemer, H. J., J. Willebrand and L. Hasse (1989), Fine adjustment of large scale air–sea energy flux parameterizations by direct estimates of ocean heat transport, *Journal of Climate,* 2, 1173–1184.

Josey, S. A., E. C. Kent, and P. K. Taylor (1998), The Southampton Oceanography Centre

612 (SOC) Ocean–Atmosphere heat, momentum and freshwater flux atlas, *Southampton*
613 *Oceanography Centre Report.*
614
615 Kara, A. B., H. E. Hurlburt, and A. J. Wallcraft (2005), Stability-dependent exchange
616 coefficients for air-sea fluxes, *Journal of Atmospheric and Oceanic Technology*, 22, 1080-1094.
617
618 Kondo, J., (1975), Air-sea bulk transfer coefficients in diabatic condition, *Boundary-Layer*
619 *Meteorology, 9,* 91–112.
620
621 Large, W. G., and S. G. Yeager (2008), The global climatology of an interannually varying air-
622 sea flux data set, *Climate Dynamics, 33,* 341-364.
623
624 Lowe, P. R (1977), An Approximating Polynomial for the Computation of Saturation Vapor
625 Pressure, *Journal of Applied Meteorology, 16*, 100–103.
626 Macdonald, A., J. Candela, and H. L. Bryden (1994), An estimate of the net heat transport
627 through the strait of Gibraltar. Seasonal and interannual variability of the western Mediterranean
628 Sea, *American Geophysical Union, 46*, 13–32.
629
630 Mariotti, A., and M. V. Struglia (2002), The hydrological cycle in the Mediterranean region and
631 implications for the water budget of the Mediterranean Sea, *Journal of Climate, 15*, 1674–1690.
632
633 Marullo, S., B. B. Nardelli, M. Guarracino, and R. Santoleri (2007), Observing the
634 Mediterranean Sea from space: 21 years of Phatfinder-AVHRR sea surface temperature (1985 to
635 2005): re-analysis and validation, *Ocean Science, 3*, 299–310.
636
637 Payne, R. E. (1972), Albedo of the sea surface, *Journal of the Atmospheric Sciences, 29*, 959-

970.

Pinardi, N., I. Allen, E. Demirov, P. De Mey, G. Korres, A. Lascaratos, P. Y. Le Traon, C. Maillard, G. Manzella, and C. Tziavos (2003), The Mediterranean ocean forecasting system: first phase of implementation (1998-2001), *Annales Geophysicae, 21*, 3–20.

Reed, R. K. (1977), On estimating insolation over the ocean, *Journal of Physical Oceanography, 7*, 482–485.

Rixen, M., J. M. Beckers, S. Levitus, J. Antonov, T. Boyer, C. Maillard, M. Fichaut, E. Balopoulos, S. Iona, H. Dooley, M. J. Garcia, B. Manca, A. Giorgetti, G. Manzella, N. Mikhailov, N. Pinardi, and M. Zavatarelli (2005), The western Mediterranean deep water: A proxy for climate change, *Geophysical Research Letters, 32*.

Rosati, A., and K. Miyakoda (1988), A general circulation model for upper ocean simulation, *Journal of Physical Oceanography*, *18*, 1601–1626.

Stammer, D., K. Ueyoshi, W. G. Large , S. Josey and C. Wunsch (2004), Estimating air–sea fluxes of heat, freshwater and momentum through global ocean data assimilation, *Journal of Geophysical Research*, 109, 1-16.

Tolmazin, D. (1985), Changing coastal oceanography of the black sea. II: Mediterranean effluent, *Progress in oceanography, 15*, 277–316.

Tonani, M., N. Pinardi, S. Dobricic, I. Pujol, and C. Fratianni (2008), A high-resolution free-surface model of the Mediterranean Sea*, Ocean Science, 4*, 1–14.

664

665 Tragou, E., and A. Lascaratos (2003), Role of aerosols on the Mediterranean solar radiation, *J.*
666 *Geophys. Res.*, *108*(C2), 3025, doi:10.1029/2001JC001258.
667

668 Uppala, S. M., P. W. Kallberg, A. J. Simmons, U. Andrae, Da, M. Fiorino, J. K. Gibson, J.
669 Haseler, A. Hernandez, G. A. Kelly, X. Li, K. Onogi, S. Saarinen, N. Sokka, R. P. Allan, E.
670 Andersson, K. Arpe, M. A. Balmaseda, A. C. M. Beljaars, Vande L. Berg, J. Bidlot, N.
671 Bormann, S. Caires, F. Chevallier1, A. Dethof, M. Dragosavac, M. Fisher, M. Fuentes, S.
672 Hagemann, E. Holm, B. J. Hoskins, L. Isaksen, P. A. E. M. Janssen, R. Jenne, Mcnally, J. F.
673 Mahfouf, J. J. Morcrette, N. A. Rayner, R. W. Saunders, P. Simon, A. Sterl8, K. E. Trenberth, A.
674 Untch, D. Vasiljevic, P. Viterbo, and J. Woollen (2005), The era-40 re-analysis, *Quarterly*
675 *Journal of the Royal Meteorological Society, 131*, 2961–3012.
676

677 Woodruff, S. D, R. J. Slutz, R. L. Jenne, and P. M. Steurer (1987), A comprehensive ocean-
678 atmosphere data set, *Bulletin of the American Meteorological Society, 68*, 1239–1250.
679

680 Xie, P., and P. A. Arkin (1996), Analyses of global monthly precipitation using gauge
681 observations, satellite estimates, and numerical model predictions, *Journal of Climate, 9*, 840-
682 858.
683

684 Yu, L., and R. A. Weller, (2007), Objectively Analyzed Air–Sea Heat Fluxes for the Global Ice-
685 Free Oceans (1981–2005), *Bulletin of the American Meteorological Society*, 88, 527–539.
686

687 Zhang, Y., W. B. Rossow, A. A. Lacis, V. Oinas, and M. I. Mishchenko (2004), Calculation of
688 radiative fluxes from the surface to top of atmosphere based on ISCCP and other global data
689 sets: Refinements of the radiative transfer model and the input data, *J. Geophys. Res.*, *109*,

690 D19105, doi:10.1029/2003JD004457.

691

Figure/Table Captions

Table 1: Heat and freshwater total fluxes and components for the period 1985-2001. The first column shows the fluxes given in the ERA-40 data set. The other six columns indicate the surface heat flux components obtained with different corrections that have been cumulatively applied.

Columns 2, 3 and 4 show the results when bulk formulas (2, 3, 7 and 8) are applied and Q_{SD} and Q_{LD} are computed according to equations 5 and 6, respectively, with no corrections in the ERA-40 input fields, corrected winds and corrected wind plus SST. The remaining columns use Q_{SD} and Q_{LD} from ISCCP-FD. Column 6 and 7 also include the humidity correction and the CMAP precipitation is included only in column 7.

Table 2: Heat and freshwater budget components for the 44-year period 1958-2001. The first column represents the values given in the original ERA-40 data set. The second column shows those obtained with the ”Corrected ERA-40 data set”, including Q_{SD} and Q_{LD}, and calculated by means of equations 2, 3, 7 and 8. Also included is the correction for ERA-40 precipitation that is obtained as the sum of convective and large-scale precipitation.

Table 3: Parameters in expressions for neutral bulk transfer coefficients

Table 4: Sensitivity of the total budget to the bulk transfer coefficient parametrization. Column 1 and 2 show total heat and freshwater fluxes and their components obtained with the ”Corrected ERA-40 data set”, including Q_{SD} and Q_{LD}, and calculated by means of equations 2, 3, 7 and 8, using Kondo (1975) and NASEC bulk transfer coefficients, respectively.

Figure 1: Surface downward shortwave radiation data. Each star represents a time average for a given station in the period 1993-2001. Blue, black and red stars are ERA-40, ISCCP- FD and AGIP data respectively. Stations have been ordered by decreasing latitudes, and their positions are located in the map. AGIP data were kindly supplied by ENI-AGIP division, Milan.

Figure 2: Wind speed correction factor R_W. The ratio is computed for the years 2000 and 2001 according to equation (9). The 2 years average QSCAT wind speed is always greater than the ERA-40 one. Values are restricted to being no greater than 1.3, because larger values are mainly due to interpolation problems in coastal areas.

Figure 3: SST correction term D_S. The difference is computed for the period 1985-2001 according to equation (10). The spatial domain is the same of the MFS OGCM, thus the correction for the Black Sea is not possible.

Figure 4: Surface solar radiation downward correction factor R_R. The ratio is computed following equation (11) for the period 1985-2001. The ISCCP-FD radiation is greater than the ECMWF reanalysis one, as demonstrated by comparison with in situ observations, with a north-west south-east gradient.

Figure 5: Specific humidity correction term D_H in g/Kg. The difference is computed for the period 1980-1993 according to equation (12).

Figure 6: Precipitation correction factor R_P. The ratio has been computed for the period 1979-2001, according to equation (13). A north-south pattern is visible in the Mediterranean Basin error field.

743 **Figure 7:** Time series of surface averaged monthly corrected T_A (A), T_S (B), q_A (C), C (D) and
744 $\left|\vec{V}\right|$ (E) with the bias reductions applied to sea surface temperature, specific humidity and wind
745 speed. The time window is 1958-2001. The mean value (solid line) and ±1 standard deviation
746 (shaded line) are also indicated.
747
748 **Figure 8:** Time series of the surface monthly averaged heat fluxes calculated with the final
749 parametrization (equations (2), (3), (7) and (8); see column 2 of tab. 2) including all the
750 mentioned corrections: Q_S (A), Q_L (B), Q_E (C), Q_H (D) and Q_T (E). The total mean (solid line)
751 and ±1 standard deviation (shaded line) are also indicated.
752
753 **Figure 9:** Climatology of Q_T $[W/m^2]$ for the month of July (A), December (B), annual (C) and
754 of F_T [m/yr] annual (D). The figures are obtained using the air sea physics which produces the
755 fluxes of tab. 2; column 2 and for the time window 1958->2001.
756
757 **Figure 10:** Panel A: Yearly averaged net surface heat flux, Q_T, (see tab 2; column 2) computed
758 with formulas (2), (3), (7) and (8) using radiative fields provided by ERA-40 and applying all the
759 corrections described in section 4. Panel B: 5-year running mean of net surface heat flux (black
760 line; left axes) and Winter (December through March) NAO index based on the difference of
761 normalized sea level pressure between Lisbon, Portugal and Stykkisholmur/Reykjavik, Iceland
762 (red line; right axes).
763
764 **Figure 11:** (a) Kondo (1975) 10 m C_E bulk transfer coefficient as a function of wind speed and
765 for 7 different T_A-T_S values; (b) 10 m C_E bulk transfer coefficient obtained from the Coupled
766 Ocean-Atmosphere Response Experiment (COARE) bulk algorithm (version 3.0) as described in
767 Fairall et al. (2003). The plot has been obtained for relative humidity equal to 80% and shows C_E
768 as a function of the wind speed for 7 different T_A-T_S values.

Tables

	ERA-40	No Corr.	+Wind	+SST	+Radiation	+Humidity	+CMAP
Q_S $[W/m^2]$	162	202	202	202	183	183	183
Q_L $[W/m^2]$	-79	-87	-87	-88	-80	-80	-80
Q_E $[W/m^2]$	-86	-80	-99	-100	-100	-91	-91
Q_H $[W/m^2]$	-10	-12	-14	-16	-16	-16	-16
Q_T $[W/m^2]$	**-13**	**24**	**2**	**-2**	**-13**	**-4**	**-4**
E [m/yr]	-1.08	-1.02	-1.27	-1.28	-1.28	-1.17	-1.17
P [m/yr]	0.39	0.39	0.39	0.39	0.39	0.39	0.47
F_T $[m/yr]$	**-0.69**	**-0.64**	**-0.89**	**-0.90**	**-0.90**	**-0.79**	**-0.70**

Table 1: Heat and freshwater total fluxes and components for the period 1985-2001. The first column shows the fluxes given in the ERA-40 data set. The other six columns indicate the surface heat flux components obtained with different corrections that have been cumulatively applied.

Columns 2, 3 and 4 show the results when bulk formulas (2, 3, 7 and 8) are applied and Q_{SD} and Q_{LD} are computed according to equations 5 and 6, respectively, with no corrections in the ERA-40 input fields, corrected winds and corrected wind plus SST. The remaining columns use Q_{SD} and Q_{LD} from ISCCP-FD. Column 6 and 7 also include the humidity correction and the CMAP precipitation is included only in column 7.

	ERA-40	**Corrected**
Q_S $[W/m^2]$	161	178
Q_L $[W/m^2]$	-78	-79
Q_E $[W/m^2]$	-86	-92
Q_H $[W/m^2]$	-10	-14
Q_T $[W/m^2]$	**-13**	**-7**
E [m/yr]	-1.08	-1.18
P [m/yr]	0.39	0.53
F_T $[m/yr]$	**-0.70**	**-0.64**

Table 2: Heat and freshwater budget components for the 44-year period 1958-2001. The first column represents the values given in the original ERA-40 data set. The second column shows those obtained with the "Corrected ERA-40 data set", including Q_{SD} and Q_{LD}, and calculated by means of equations 2, 3, 7 and 8. Also included is the correction for ERA-40 precipitation that is obtained as the sum of convective and large-scale precipitation.

$\left\|\vec{V}\right\|$ $[m/s]$	a_h	a_e	b_h	b_e	c_h	c_e	p_h	p_e
0.3 to 2.2	0	0	1.185	1.23	0	0	-0.157	-0.16
2.2 to 5	0.927	0.969	0.0546	0.0521	0	0	1	1
5 to 8	1.15	1.18	0.01	0.01	0	0	1	1
8 to 25	1.17	1.196	0.0075	0.008	-0.00045	-0.0004	1	1
25 to 50	1.625	1.68	-0.017	-0.016	0	0	1	1

Table 3: Parameters in expressions for neutral bulk transfer coefficients.

	Kondo	**NASEC**
Q_S $[W/m^2]$	182	182
Q_L $[W/m^2]$	-79	-79
Q_E $[W/m^2]$	-94	-86
Q_H $[W/m^2]$	-14	-13
Q_T $[W/m^2]$	**-5**	**4**
E [m/yr]	-1.20	-1.10
P [m/yr]	0.53	0.53
F_T $[m/yr]$	**-0.67**	**-0.57**

799

800 **Table 4:** Sensitivity of the total budget to the bulk transfer coefficient parametrization. Column
801 1 and 2 show total heat and freshwater fluxes and their components obtained with the "Corrected
802 ERA-40 data set", including Q_{SD} and Q_{LD}, and calculated by means of equations 2, 3, 7 and 8,
803 using Kondo (1975) and NASEC bulk transfer coefficients, respectively.

804

805

Figures

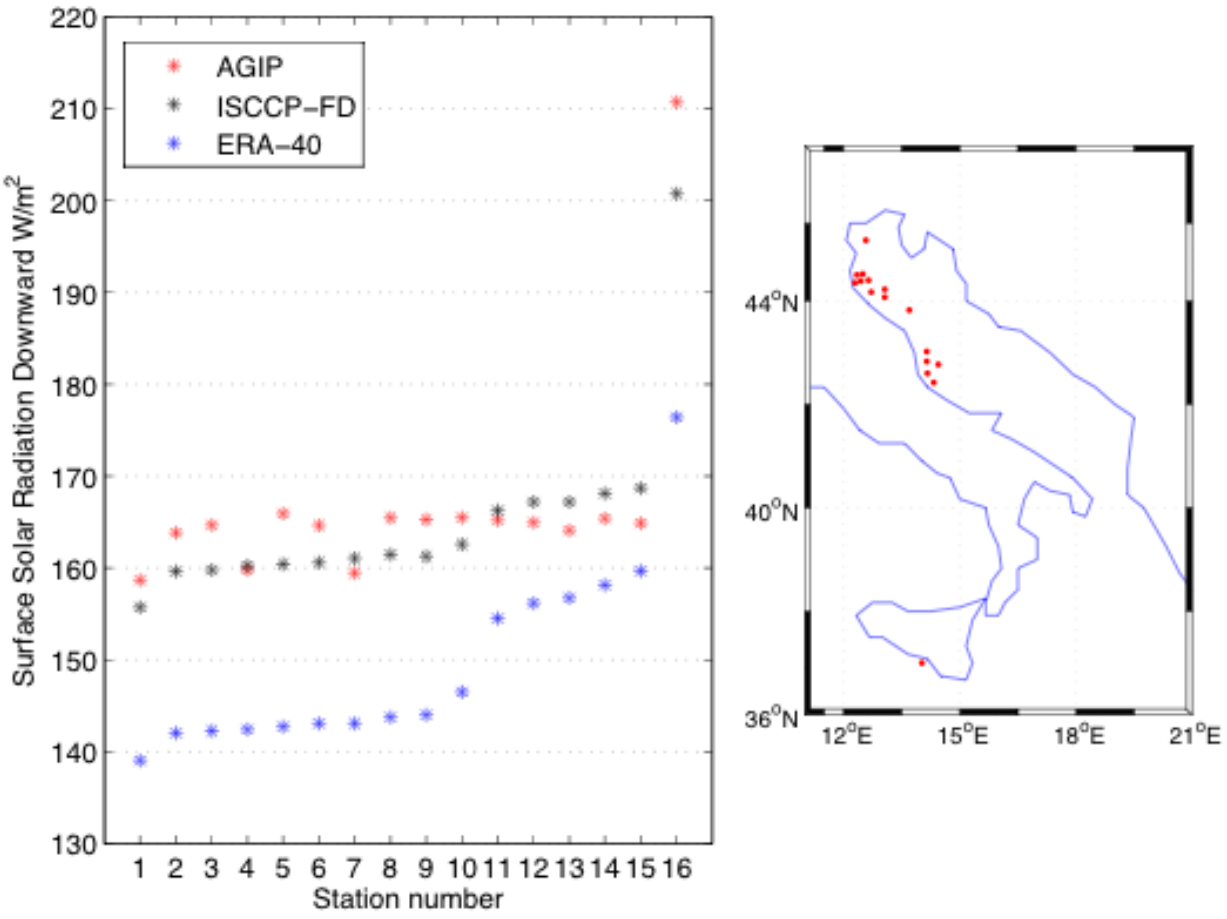

Figure 1: Surface downward shortwave radiation data. Each star represents a time average for a given station in the period 1993-2001. Blue, black and red stars are ERA-40, ISCCP- FD and AGIP data respectively. Stations have been ordered by decreasing latitudes, and their positions are located in the map. AGIP data were kindly supplied by ENI-AGIP division, Milan.

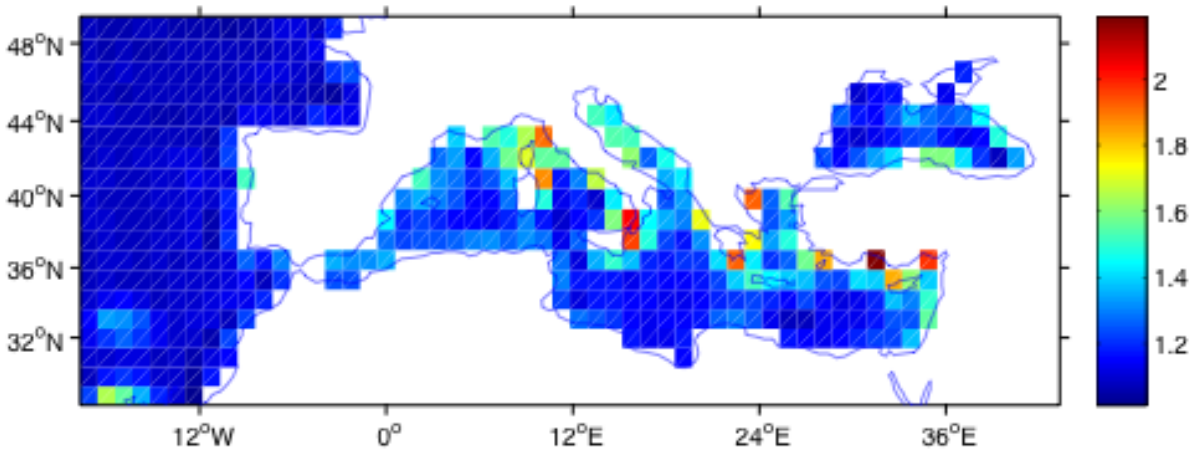

Figure 2: Wind speed correction factor R_W. The ratio is computed for the years 2000 and 2001 according to equation (9). The 2 years average QSCAT wind speed is always greater than the ERA-40 one. Values are restricted to being no greater than 1.3, because larger values are mainly due to interpolation problems in coastal areas.

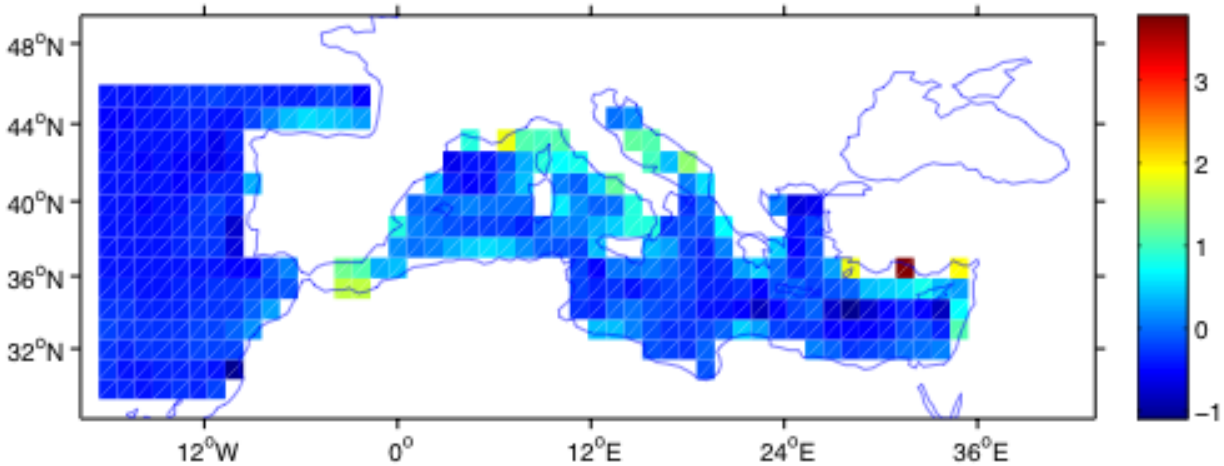

Figure 3: SST correction term D_S. The difference is computed for the period 1985-2001 according to equation (10). The spatial domain is the same of the MFS OGCM, thus the correction for the Black Sea is not possible.

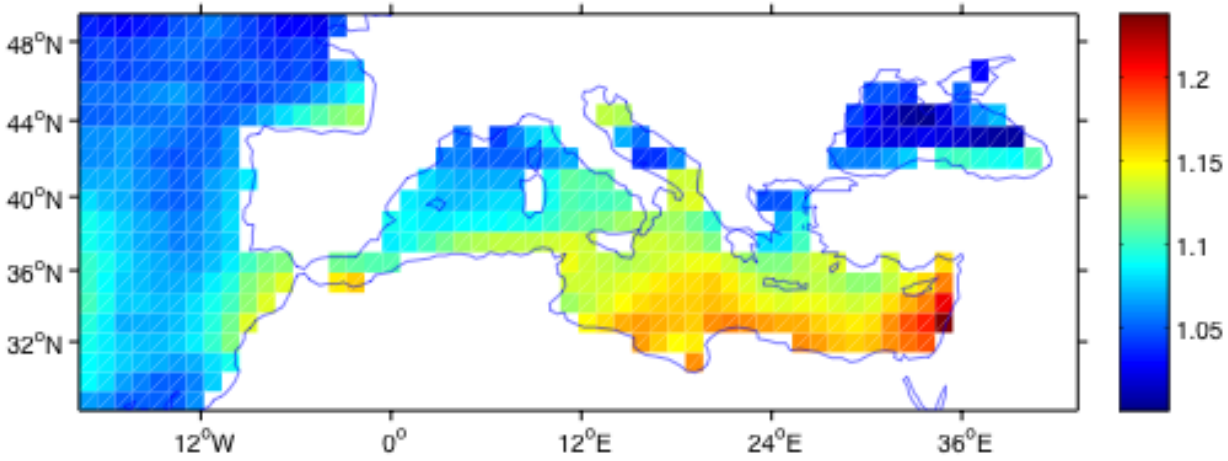

Figure 4: Surface solar radiation downward correction factor R_R. The ratio is computed following equation (11) for the period 1985-2001. The ISCCP-FD radiation is greater than the ECMWF reanalysis one, as demonstrated by comparison with in situ observations, with a north-west south-east gradient.

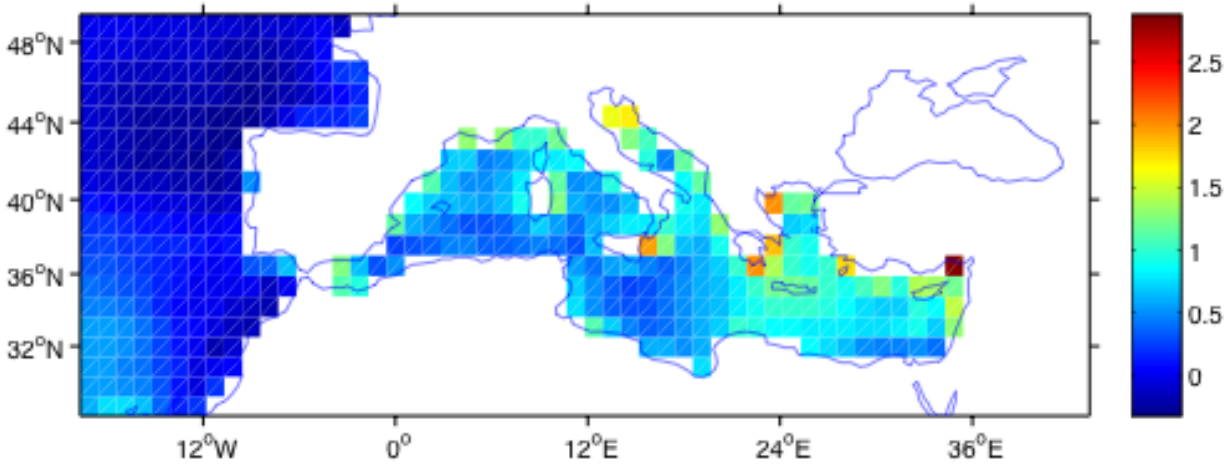

Figure 5: Specific humidity correction term D_H in g/Kg. The difference is computed for the period 1980-1993 according to equation (12).

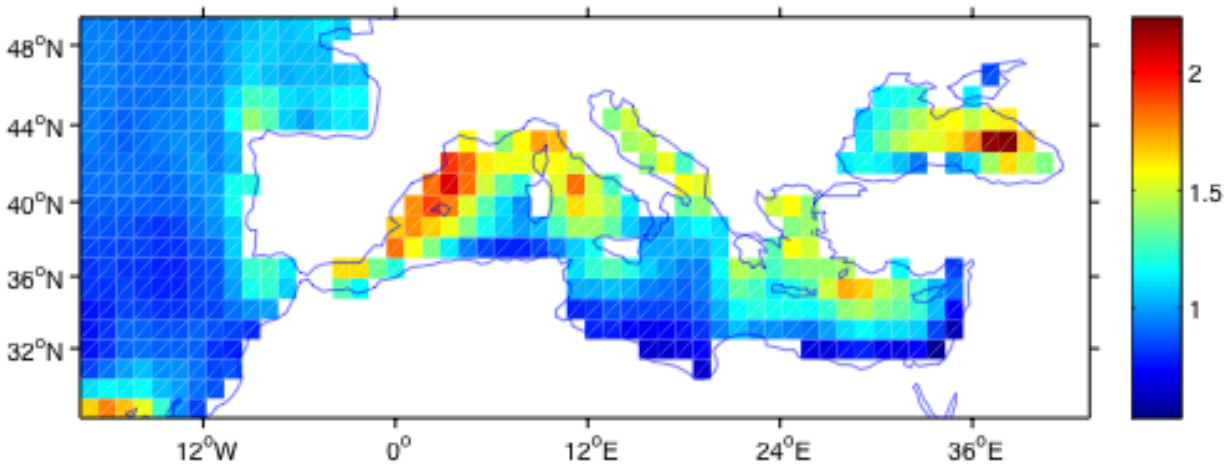

Figure 6: Precipitation correction factor R_P. The ratio has been computed for the period 1979-2001, according to equation (13). A north-south pattern is visible in the Mediterranean Basin error field.

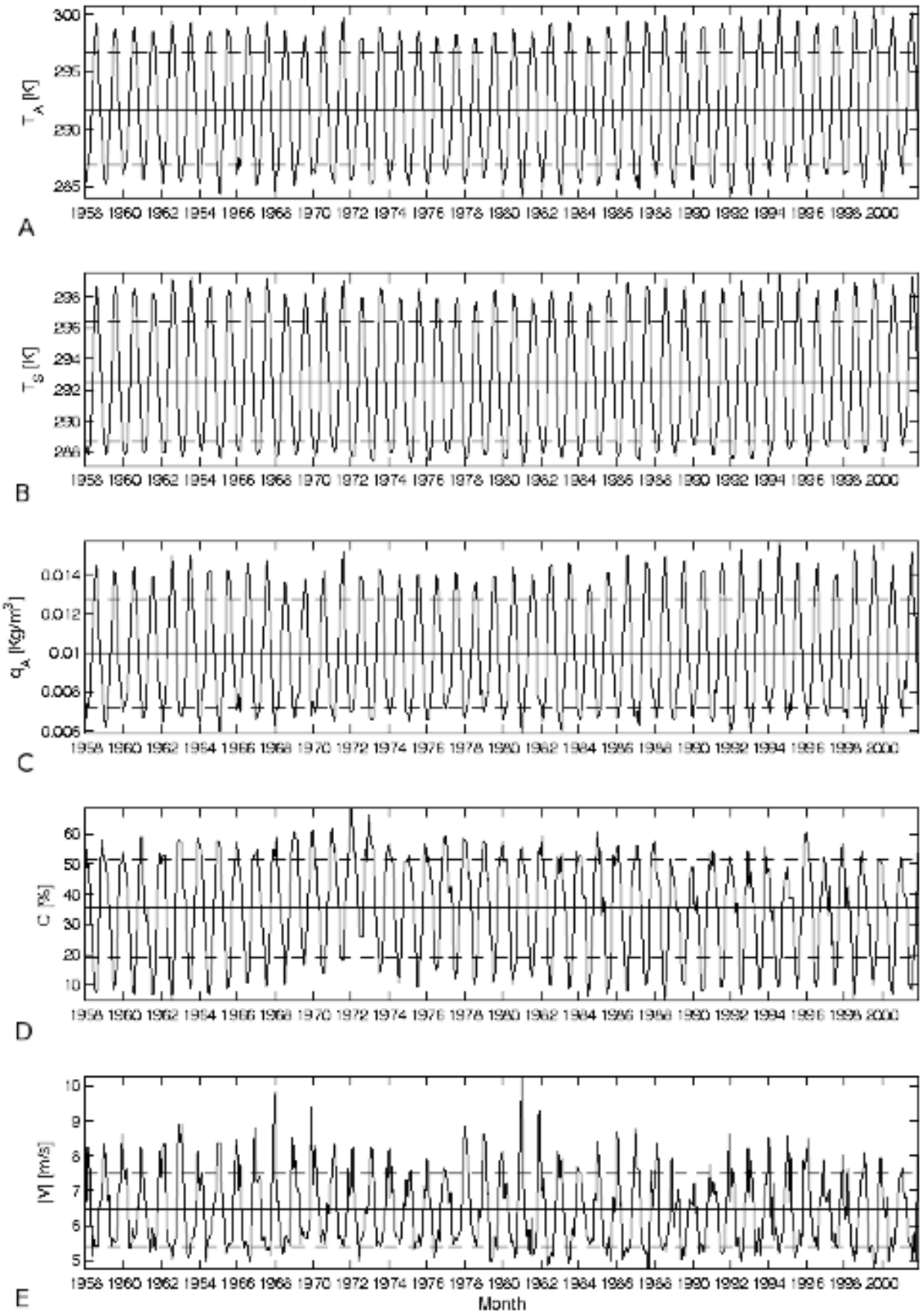

Figure 7: Time series of surface averaged monthly corrected T_A (A), T_S (B), q_A (C), C (D) and $\left|\vec{V}\right|$ (E) with the bias reductions applied to sea surface temperature, specific humidity and wind speed. The time window is 1958-2001. The mean value (solid line) and ±1 standard deviation (shaded line) are also indicated.

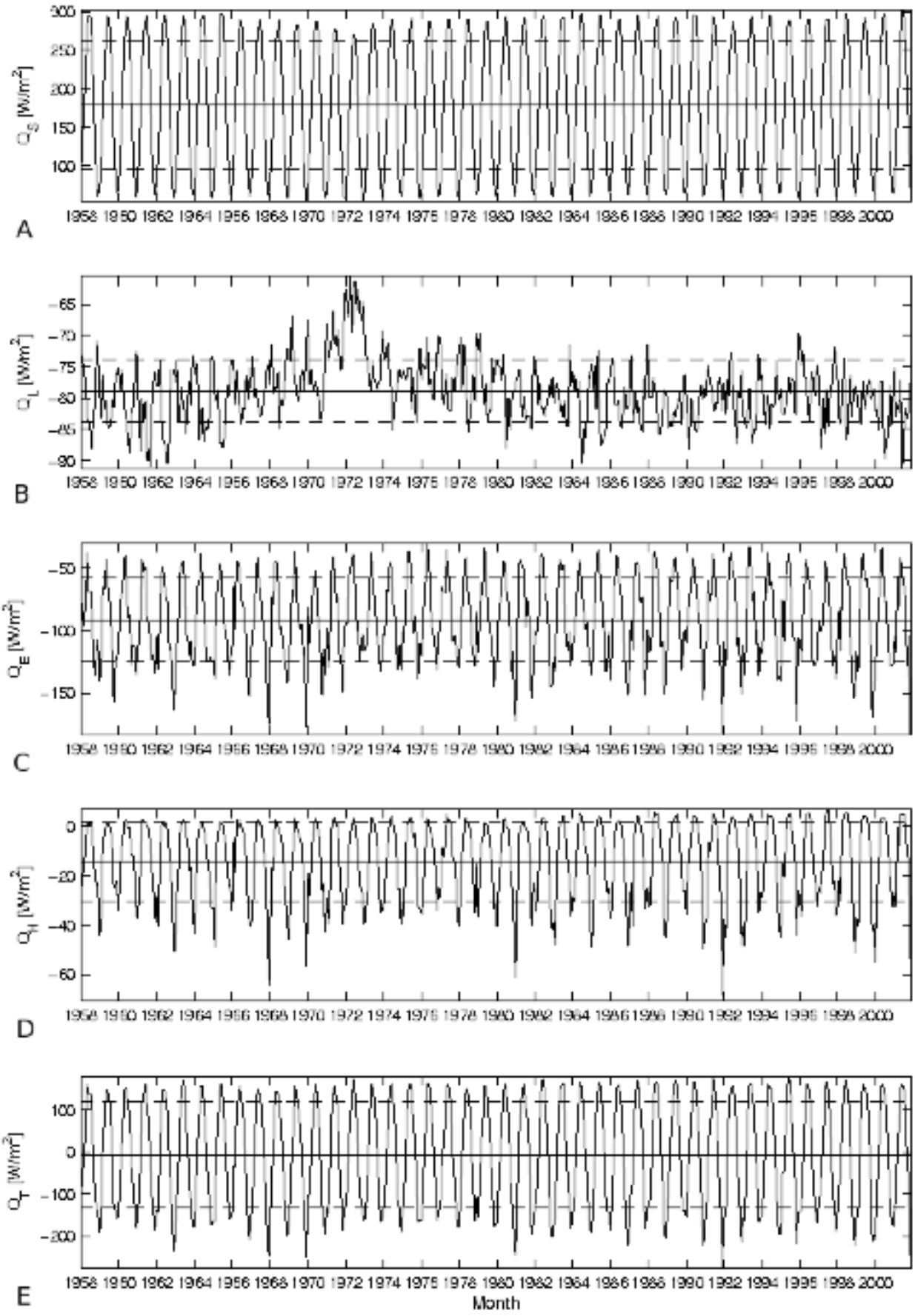

Figure 8: Time series of the surface monthly averaged heat fluxes calculated with the final parametrization (equations (2), (3), (7) and (8); see column 2 of tab. 2) including all the mentioned corrections: Q_S (A), Q_L (B), Q_E (C), Q_H (D) and Q_T (E). The total mean (solid line) and ±1 standard deviation (shaded line) are also indicated.

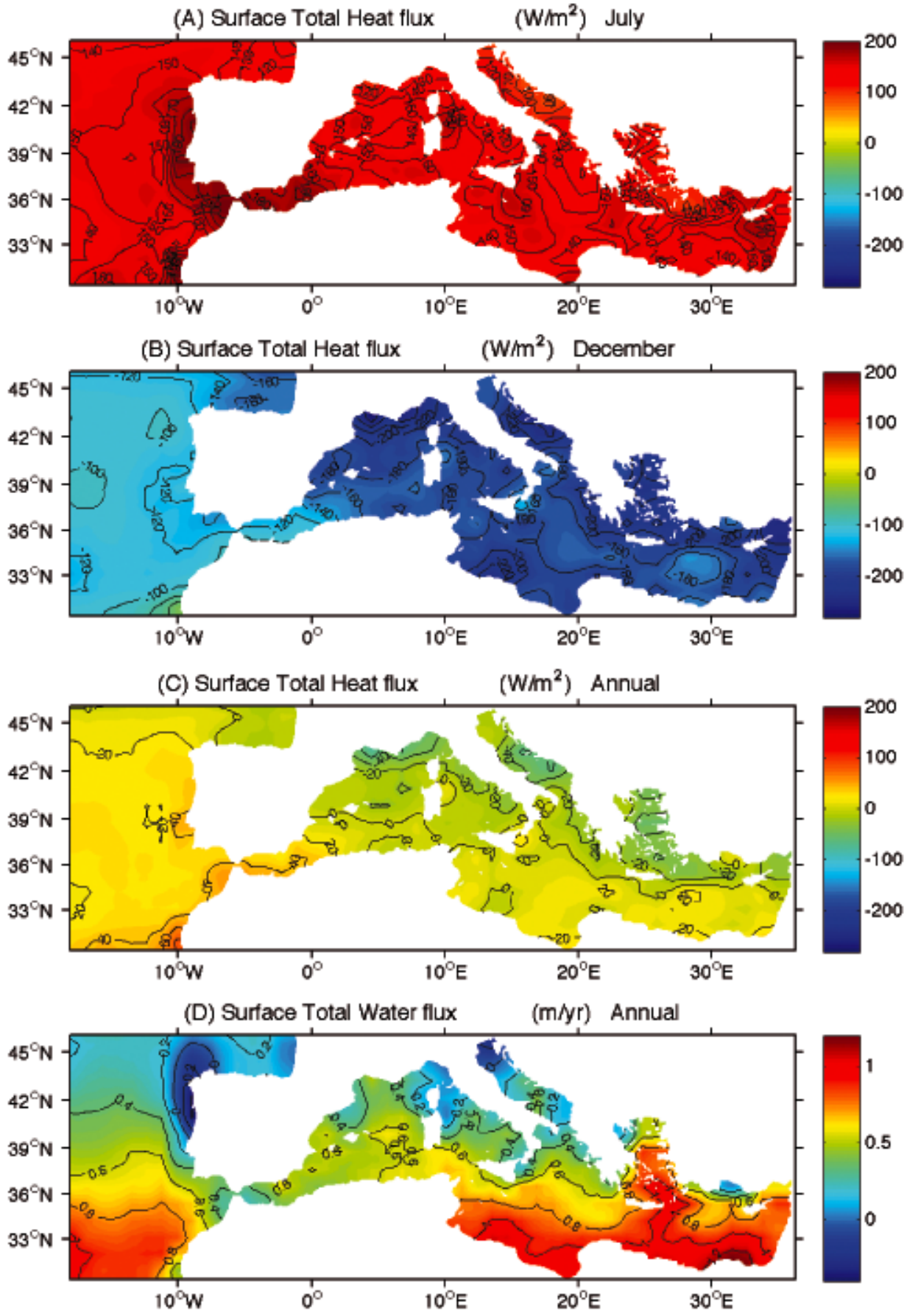

Figure 9: Climatology of Q_T $[W/m^2]$ for the month of July (A), December (B), annual (C) and of F_T [m/yr] annual (D). The figures are obtained using the air sea physics which produces the fluxes of tab. 2; column 2 and for the time window 1958->2001.

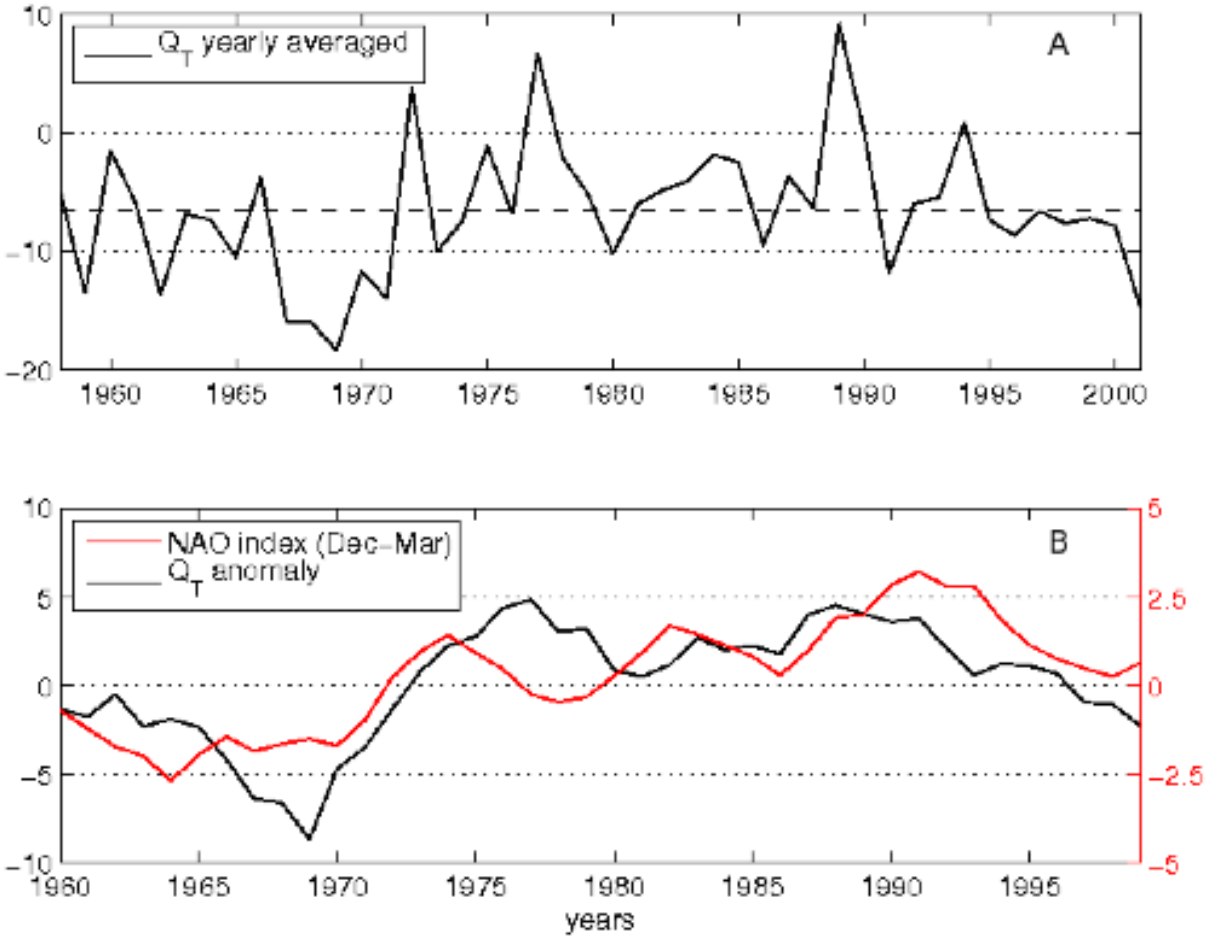

Figure 10: Panel A: Yearly averaged net surface heat flux, Q_T, (see tab 2; column 2) computed with formulas (2), (3), (7) and (8) using radiative fields provided by ERA-40 and applying all the corrections described in section 4. Panel B: 5-year running mean of net surface heat flux (black line; left axes) and Winter (December through March) NAO index based on the difference of normalized sea level pressure between Lisbon, Portugal and Stykkisholmur/Reykjavik, Iceland (red line; right axes).

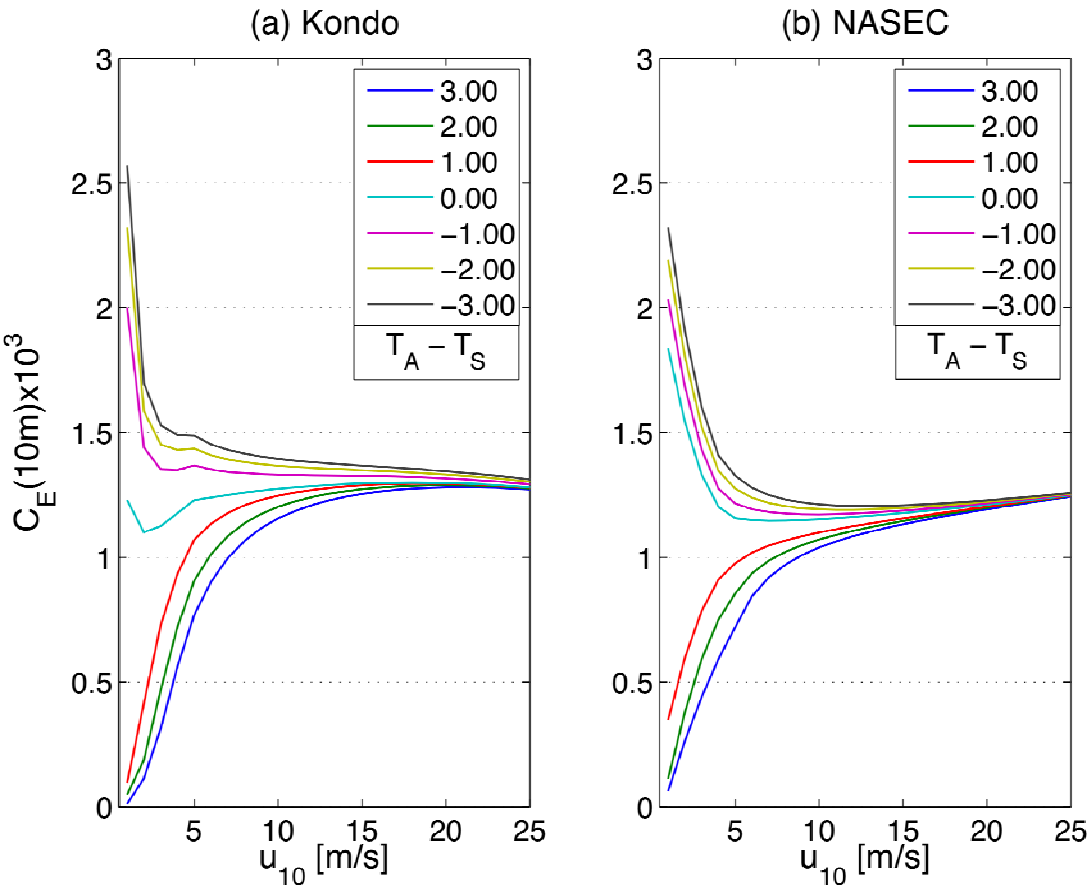

Figure 11: (a) Kondo (1975) 10 m C_E bulk transfer coefficient as a function of wind speed and for 7 different T_A-T_S values; (b) 10 m C_E bulk transfer coefficient obtained from the Coupled Ocean-Atmosphere Response Experiment (COARE) bulk algorithm (version 3.0) as described in Fairall et al. (2003). The plot has been obtained for relative humidity equal to 80% and shows C_E as a function of the wind speed for 7 different T_A-T_S values.